SHOCK-DARKENING IN ORDINARY CHONDRITES: MODELING OF THE PRESSURE-TEMPERATURE CONDITIONS. J. Moreau[1], T. Kohout[1,2] and K. Wünnemann[3], [1]Department of Physics, University of Helsinki, Finland (juulia.moreau@helsinki.fi), [2]Institute of Geology, The Czech Academy of Sciences, Prague, Czech Republic, [3]Museum für Naturkunde, Leibniz Institute for Evolution and Biodiversity Science, Berlin, Germany.

Introduction: Shock-darkening in ordinary chondrites is the partial melting of metals and iron sulfides filling cracks within silicate grains [1-5]. Shock-darkening leads to optical darkening, making asteroids classification more difficult ([6], [7]). In such cases, S-type asteroids (chondritic silicate composition) spectra look like C-type asteroids (associated with carbonaceous chondrites).

Methods: To study the pressure and temperature conditions at which this process occurs, we used the shock physics code iSALE [8, 9]. The mesoscale approach of a planar shock wave in 2D is used, implementing four olivine layers (Fig. 1):

- A Flyer plate, from which the shock wave is generated
- A top buffer plate, giving the nominal pressure, the proxy of this study.
- A sample plate with 2 sorts of particles: iron and troilite.
- A bottom buffer plate.

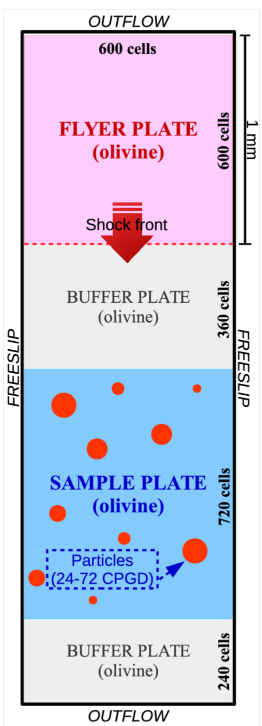

Fig 1. Numerical setup. CPGD stands for: cells per grain diameter.

Olivine was described by ANEOS (analytical equation of state, [10], [11]) and had a porosity of 6%. Iron was described by ANEOS and Troilite by a Tillotson EOS [12] (using pyrrhotite [13]).

Porosity. There is two ways to represent porosity in iSALE:

- As a material input parameter (ε-α compaction model [8] with distension $\alpha = 1 / (1-\Phi)$ where Φ is the porosity fraction)
- With resolved individual pores [14] and no additional particles.

Post-shock temperatures (PSTs). To study the melt fraction, we used PSTs relative to the peak shock pressures. At release, residual energy is translated to post-shock temperatures. We used a linear relationship: $U = C + S.u_p$, with u_p, particle velocity and U, shock-wave velocity, and a series of dedicated equations to compute PSTs for troilite and the other materials [15-17]. Using tracers, we recorded the peak shock pressures in each material from which PSTs were calculated and melt fractions assessed [18].

Results: We ran two sets of models with each type of ordinary chondrites (H, L and LL). The first set of results used porous olivine (ε-α compaction model). The second set of results used a non-porous olivine to which an olivine melt profile from an additional model using pores was added. The iron/troilite particles distribution followed data from [19].

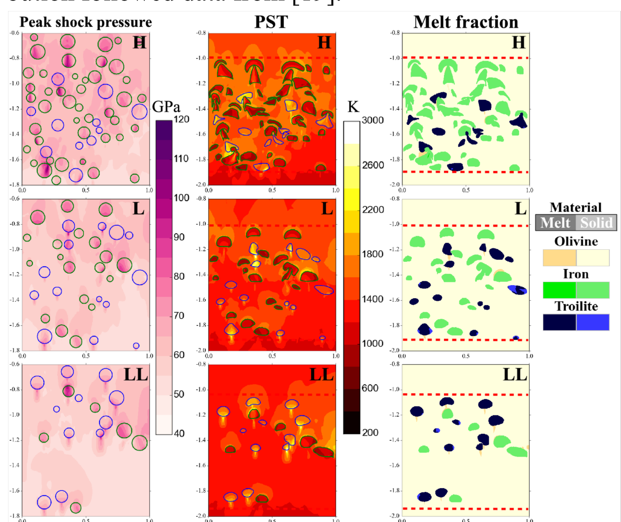

Fig 2. Results of the OCs mesoscale models showing the sample plates (delineated by the red dashed line at release) and particles (iron: green, troilite: blue in P/T panels). The peak shock pressures are shown in a non-compressed sample plate. All panels are at the same nominal pressure (51 GPa) but the generated peak shock pressures are different due to the strong reflections between olivine and iron/troilite grains (H-OC: 64 GPa, L-OC: 60 GPa, LL-OC: 58 GPa). Panels graduations are in mm and PST stands for Post-shock temperatures.

In Fig. 2 is shown an example of release states of H, L and LL ordinary chondrites at 51 GPa of nominal pressure. In Fig. 3, are shown profiles of the materials melts for the first set of models. For each material:

- Troilite starts to melt at ~40 GPa to complete melt at 50 GPa of nominal pressure. It melted as a consequence of shock wave-induced increase in entropy (pure shock melting) and is rarely influenced by reflexions when reaching peak shock pressures.

- Iron starts to melt at 50-58 GPa of nominal pressure to a few percents only. If melting, it is mainly due to strong reflections or specific disposition of the particles (~elongated grains).
- Olivine starts to melt at ~50 GPa of nominal pressure and this is due to strong reflexions at iron grains boundaries, rising the peak shock pressure and thus PSTs.

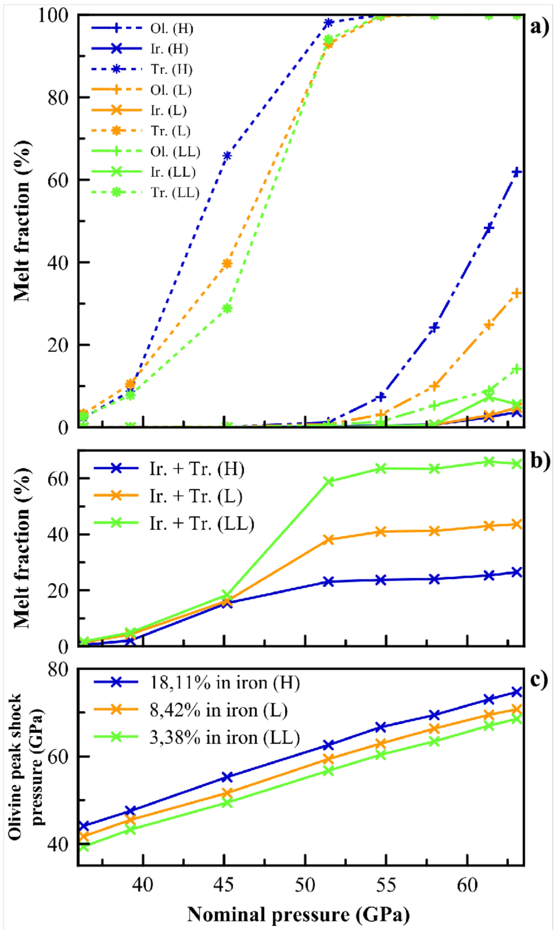

Fig 3. Results of the OC mesoscale models with porous olivine and a) melt fractions for each material after pressure release in each OC type, b) combined iron and troilite melt-fraction to reflect the grain distribution and total shock-darkening melt phases and c) generated peak shock pressures in olivine in regard of the iron grains abundance. Each OC is represented by its abbreviation and phases are Ir.: iron, Tr.: troilite, Ol.: olivine.

Discussion: Our results show that shock-darkening happens at pressures from 40 GPa to 50 GPa at the complete melt of troilite and onset of olivine melt. We observe that the influence of iron is important for olivine (Fig. 3c) and that the shock-darkening agent is only composed of troilite. In our models, we did not consider heat transfer after release and no Fe-FeS eutectic point (unshocked petrologies show only few Fe-FeS mixtures) - melting temperatures for the materials were therefore higher. No shearing between grains was considered and the PSTs calculation is a crude estimate for olivine due to the many reflections inside the sample.

Conclusion: Based on numerical modeling, the shock-darkening process in ordinary chondrites starts at 40 up to 50 GPa. In each ordinary chondrites type, troilite melts completely, leading to the optical darkening when filling the cracks. Heat transfer, shearing and the eutectic point would all lower the resulting pressures and is subject to future work.

Acknowledgments: Our thanks go to the team of the Museum für Naturkunde in Berlin, Germany, for sharing their knowledge and ideas with us. This work is also supported by the Academy of Finland.

References: [1] Heymann D. (1967) *Icarus*, 6, 189-221. [2] Britt D. T. et al. (1989) Proc. *19th LPSC*, 537-545. [3] Britt D. T. and Pieters C. M. (1989) Proc. *20Th LPSC*, 109-110. [4] Britt D. T. and Pieters C. M. (1994), *Geochim. Cosmochim. Acta*, 58(18), 3905-3919. [5] Kohout T. et al. (2014) *Icarus*, 228, 78-85. [6] DeMeo F. E. et al. (2009) *Icarus*, 202, 160-180. [7] DeMeo F. E. and Carry R. P. (2014) *Nature*, 505, 629-634. [8] Wünnemann K. et al. (2006) *Icarus*, 180, 514-527. [9] Moreau J. et al. (2017) **MAPS**, submitted[10] Thompson S. L. (1990) *Comp. Phys. Mech. Div, I, Sandia Nat, Lab*. [11] Melosh H. J. (2007) *MAPS*, 42(12), 2079-2098. [12] Tillotson J. H. (1962) *Gen. Atom. Div. Of Gen. Dyn*. [13] Ahrens T. J. (1979) *JGR*, 84(B3), 985-998. [14] Güldermeister N. et al. (2013) MAPS, 48(1), 115-133. [15] Artemieva N. and Ivanov B. (2004) *Icarus*, 171, 84-101. [16] Fritz J. et al. (2005) *Meteoritics & Planet. Sci.*, 40, 9/10, 1393-1411. [17] Watters W. A. et al. (2009) *JGR*, 114, E02001. [18] Wünnemann K. et al. (2008) EPSL, 269, 529-538. [19} McSween Jr. H. Y. et al. (1991) Icarus, 90(1), 107-116.